Available online at www.sciencedirect.com

ScienceDirect

journal homepage: www.elsevier.com/locate/ajps

Original Research Paper

Enhanced dissolution of poorly soluble antiviral drugs from nanoparticles of cellulose acetate based solid dispersion matrices

Sonal Mazumder [a], *Ashish Kumar Dewangan* [a], *Naresh Pavurala* [b,*]

[a] *Department of Chemical Engineering, Birla Institute of Science and Technology, Pilani, Rajasthan 333031, India*
[b] *Oak Ridge Associated Universities, Food and Drug Administration, Silver Spring, MD, USA*

ARTICLE INFO

Article history:
Received 3 April 2017
Received in revised form 9 June 2017
Accepted 3 July 2017
Available online 8 July 2017

Keywords:
Solid dispersions
Ritonavir
Efavirenz
Nanoparticles
Precipitation
Solubility

ABSTRACT

Polysaccharide-based polymers were used to produce nanoparticles of poorly soluble antiviral drugs using a rapid precipitation process. The structure-property relationships of four novel cellulose acetate-based polymers were studied for their solubility enhancement of poorly soluble drugs. Particles were purified by dialysis, and dried powders were recovered after freeze-drying. The particle diameters were 150–200 nm. The target drug loading in the particles was 25 wt%, and the drug loading efficiencies were 80–96%. The effects of the formulation process and nanoparticle properties on drug solubility were investigated. All nanoparticles afforded increased solubility and faster release compared to pure drugs. Drug release was a function of the relative hydrophobicity (or solubility parameters) of the polymers.

1. Introduction

Oral administration of therapeutic agents is the easiest, and often most preferred, mode of drug delivery, as there is no requirement for hospitalization that requires medical infrastructure, a critical issue in underdeveloped countries. In addition, patient compliance in taking oral medications is greater than for injected formulations [1]. However, it is vital to attain the desired pharmacokinetic profile for a given drug, especially one with poor aqueous solubility [2] . The GI tract has several tissue barriers (mucosa, microvilli) and physiological factors (varying pH, enzymes, transporter mechanisms), which limit the bioavailability of drugs in the intestine [3]. The drug bioavailability is ultimately controlled by the rate-limiting step, which is its dissolution.

Several possible strategies could be employed to increase the bioavailability of poorly soluble drugs, such as ionized salts addition, solid dispersions, micronization and soft gel technology [4]. However, there are some inherent limitations associated with these techniques such as drug-loading capacity, toxicity, biodegradability, large dosages and environmental

* *Corresponding author.* Oak Ridge Associated Universities, Food and Drug Administration, Silver Spring, MD 20740, USA. Tel.: + 301 796 4207.
E-mail address: naresh.pavurala@fda.hhs.gov (N. Pavurala).
Peer review under responsibility of Shenyang Pharmaceutical University.
https://doi.org/10.1016/j.ajps.2017.07.002

considerations. In the recent years, nanotechnology has emerged as a promising field to address these issues [5]. Nanoparticles with well-defined size distributions have the potential to release large fractions of their drug load in the first few hours in the small intestine.

Many polymeric materials have been used for this purpose, such as poly(lactic acid), poly(glycolic acid), polycaprolactone, polysaccharides, the poly(acrylic acid) family, proteins and polypeptides (e.g., gelatin) [6]. Among these, polysaccharides are recently the most popular nanoparticle materials for drug delivery. Polysaccharides are complex carbohydrate polymers consisting of more than 2 monosaccharides linked together covalently by glycosidic linkages in a condensation reaction. Cellulose is the most abundant polysaccharide found in nature. It is a linear polymer consisting of 6-member ether rings (D-glucose or dextrose) linked together covalently by ether groups, the so-called glycosidic bonds. Usually, many thousand glucose repeat units make up a cellulose polymer. Cellulose derivatives are chosen as they are amenable to chemical modification and are biologically compatible, and particular derivatives have been shown to improve the amount of drug solubilized through stabilizing the amorphous form.

As stated before, the amorphous form of the drug requires less energy for dissolution due to a lack of crystalline lattices and thus exhibits higher bioavailability than the crystalline form. This leads to the introduction of an amorphous solid dispersion (ASD). ASDs are formed when the drug is evenly and molecularly dispersed in an amorphous polymer matrix. The drug is in the amorphous form in the matrix. ASDs are particularly interesting for many poorly soluble drugs because they offer many advantages such as faster dissolution rates and higher drug concentrations in the gastrointestinal milieu [7]. Higher dissolution rates may lead to significant improvements in drug absorption [8–12].

To form an amorphous matrix of drug and polymer, polymers must possess certain properties; they must be nontoxic, miscible with the (often hydrophobic) drug and must have a trigger mechanism for drug release, such as pH sensitivity. The polymer must possess a high glass transition temperature so that the formulation can be transferred and stored for months. A high glass transition temperature indicates greater stability. The polymer must not itself have a tendency to crystallize [13,14]. It is preferable that the crystallinity of the drug substance be suppressed by the polymer carrier, since it can act as a seed, resulting in additional crystal growth and ultimately a reduced shelf-life for the drug formulation [15] . To date, polymers used in pharmaceutical formulations such as polyethylene glycol (PEG) and poly(vinylpyrollidinone) PVP have been used to enhance drug solubility. However, these polymers have certain limitations, such as high water solubility, a tendency to crystallize and an inability to stabilize some active ingredients in the solid phase [16].

Recently, cellulose esters have been shown to be very promising for oral drug delivery, due to their affinity for complexing with a variety of drugs, ability to suppress crystallization of the drugs, relatively high glass transition temperatures and biocompatibility [17]. Recently, another interesting polysaccharide, hydroxypropylmethyl cellulose acetate succinate (HPMCAS), has been shown to have interesting properties and to form amorphous matrix formulations [18] . Though several studies have investigated the formulation of polymer-antiviral drug nanoparticles with synthetic or semisynthetic polymers [19–23], natural polysaccharides have not been explored as anti-HIV nanocarrier systems. In our work, for the first time, an amorphous solid dispersion of polymer-drug nanoparticles was prepared using a rapid precipitation process. It was hypothesized that the effect of synergy between ASD and particle size reduction will lead to a high release rate in the small intestine, which could further improve the solution concentration and bioavailability and reduce the required dose.

In this work, two poorly soluble antiviral drugs, ritonavir (RTV) and efavirenz (EFV), with solubility of 1.2 μg/L and 8.85 μg/L at pH 6.8, respectively, were chosen for the study. Comparatively novel cellulose acetate-based polymers were chosen to prepare the nanoparticles. All contain pendant carboxyl groups and are thus pH-sensitive and water-swellable when partially ionized at pH 6–7 but insoluble at pH ~ 3–4 [17]. No previous study has reported these drugs complexed with these polysaccharides to form nanoparticles. The effect of processing conditions on the particle size and drug loading of nanoparticles of RTV and EFV, made with these polysaccharides using the flash nano-precipitation method, was investigated [17,24–26] in a multi-inlet vortex mixer (MIVM) [27–30]. With this method, nanoparticles form very rapidly through controlled nucleation and growth of particles, which allows for the production of nanoparticles of controlled size in a continuous manner [31].

Particle size and drug loading was studied thoroughly to test the reproducibility of the particle formation process. Drug release and solution concentration were studied, and the effects of the structure-property relationship of the polymers and their nanoparticle properties were established.

2. Materials and methods

2.1. Materials

Tetrahydrofuran (anhydrous, ACS reagent, ≥99.0% inhibitor free, MOLYCHEM, India) was used as received. Acetonitrile (HPLC grade, >95 %, MOLYCHEM, India) was used for HPLC analysis without further purification. RTV and EFV (Sigma Aldrich, India) were used without further purification. The polysaccharides were samples from the Eastman Chemical Company and the derivatives were prepared using established methods [32]. Millipore water (18.2 MΩ•cm at 25 °C ultrapure) was used for all experiments. Dialysis tubing (Spectropore, cellulose ester) used for solvent removal had a molecular weight cut-off (MWCO) of 25K. D-(+)-Trehalose dehydrate (Sigma Aldrich, CAS 6138-23-4, molecular weight – 378.33 g/mole) was used as a cryoprotectant against aggregation during freeze-drying. The abbreviations used in this paper for novel polymers used in this work, along with some of their properties, are presented in Table 1.

2.2. Methods

2.2.1. *Nanoparticle preparation by rapid precipitation in the multi inlet vortex mixer*

Flash nanoprecipitation of polymer-drug complexes was performed in a four-jet Multi-Inlet Vortex Mixer that accommodates

Table 1 – Abbreviation and properties of novel cellulose derivatives.

Polymer	Polymer abbreviation	DS (CO_2H)	DS (other)	DS (total)	Solubility parameter ($MPa^{1/2}$)	Molecular weight ($\times 10^3$)	T_g (°C)
Carboxymethyl Cellulose Acetate Butyrate	CMCAB	0.33	Ac 0.44; Bu 1.64	2.41	23.18	22	137
Cellulose Acetate Propionate 504-0.2 Adipate 0.33	CAP Adp 0.33	0.33	Ac 0.04; Pr 2.09	2.46	20.56	12.0	125
Cellulose Acetate Propionate Adipate 0.85	CAP Adp 0.85	0.85	Ac 0.04; Pr 2.09	2.98	21.27	9.7	110
Cellulose Acetate 320S Sebacate	CA 320S Seb	0.57	Ac 1.82	2.39	22.36	25	117

DS = Degree of substitution; Tg (°C) = Glass transition temperature.

four streams, as described in our previous study [33,34]. The polymer and drug (RTV/EFV) were dissolved in THF (organic stream), which was injected into the mixer with three other water streams. The four inlet streams were tangential to the mixing chamber and the exit stream emerged from the center of the chamber. The nanoparticles formed at a nominal Reynolds number of 5000. The injected volume ratio of THF to Millipore water was 1:10 v/v. The polymer concentration in THF was 10 mg/ml. The effect of the loading of the RTV and EFV was investigated with a target loading of 25 wt% of total solids on a dry basis. The effect of drug loading on the release of drug from the polymer nanoparticles was explored.

2.2.2. *Microparticle formation*

Ritonavir drug/polymer microparticles were prepared for comparison. Polymers (150 mg) in 40 ml acetone were stirred at room temperature until the polymer was completely dissolved (approximately 2 h). Ritonavir (50 mg) was added to this solution and stirred for 10 min. The acetone solution containing the dissolved polymer and drug was added dropwise to 150 ml of water. The organic solvent was removed from the resulting suspension using a rotary evaporator. The resulting aqueous solution was then freeze-dried to yield microparticles of amorphous solid dispersions of ritonavir/polymers.

2.2.3. *Nanoparticles recovery, solvent removal and drying*

Since the particles exit the MIVM in a mixed organic-water phase, it is necessary to remove the solvent and any unincorporated drug from the particles. Thus, particles were processed by dialysis followed by freeze-drying. The dialyzed particles were dried in a Scanvac, Coolsafe 55-4 Pro freeze dryer at 0.45–0.52 mbar for 24 h.

2.2.4. *Drug composition by HPLC*

Drug loading and drug release were measured using an Agilent 1200 Series HPLC system, which consisted of a quaternary pump, online degasser, manual injector with a 20-µl sample loop and Agilent Chemstation LC 3D software. Chromatography was conducted in reverse mode using acetonitrile and phosphate buffer (0.05 M, pH 5.65). A gradient at 40% for 1 min, raised to 60% in 14 min, was reduced to 40% in 1 min and held at 40% for 4 min. Total analysis time was 20 min. Mobile phase flow rate was 1.5 ml/min, with a column temperature at 30 °C and a sample injection volume of 5 µl. Detection was performed with a diode array detector at 240 nm for RTV and EFV. The drug concentration was obtained from calibration curves for RTV and EFV.

2.2.5. *Particle size – dynamic light scattering and scanning electron microscopy*

The particle size and polydispersity index were found with a dynamic light scattering (DLS) technique using Zetasizer (ModelZEN 3602, Malvern Corp, UK) equipped with Zetasizer software. The measurements were made at a fixed light scattering angle of 173°. Distilled water was used as the dispersing solvent for dilution before every measurement. Zeta potential measurements were also conducted in the same cuvette cells. The Smoluchowski approximation was selected as the f(Ka) parameter because particles are dispersed in aqueous medium. The temperature for all measurements was set as 25 °C. All measurements were carried out 12 times per sample.

For DLS analysis of the complexes, typically 200 µl of the nanoparticle suspension obtained from the mixer were diluted with 2 ml of deionized water. The dialyzed suspensions (1 ml) were diluted with 3 ml of deionized water and the freeze-dried powders were diluted with deionized water to a concentration of 0.1 mg/ml. Trehalose was added before freezing (as a cryoprotectant) in a ratio of nanoparticles: trehalose = 1:10 to control the stability of the particles. Trehalose forms hydrogen bonds with nanoparticles during freeze drying. It is less hygroscopic, with low chemical reactivity and a high glass transition temperature [34]. Therefore, it was used as a suitable cryoprotectant in this work. The suspensions were sonicated in a bath sonicator (Johnson Plastosonic, 20KHz) for 10 min before measuring particle size by dynamic light scattering.

Field emission scanning electron microscope (FESEM) images of the microparticles were obtained using an LEO (Zeiss) 1550 instrument at a 5 kV accelerating voltage in the conventional high vacuum mode. The microparticles were sonicated at 0.01 mg/ml in DI water. Approximately 100 µl of the prepared samples was placed on imaging tape and allowed to dry at room temperature. Samples for SEM were mounted on metal stubs and coated with gold prior to analysis.

2.2.6. *Characterization of crystallinity*

Crystallinity of nanoparticles was evaluated by powder X-ray diffraction (PXRD) and differential scanning calorimeter (DSC). PXRD patterns were obtained using a Rigaku Mini Flex-II fitted with a Cu K source. The X-ray tube consists of a target material made of copper, which emits Kα radiation (λ = 1.54 A°) using a power rating of 2200 watts and an accelerating potential of 60 kV. The divergence and scattering slits were set at 1.0° and the receiving slit was at 0.1 mm. The experiment was conducted with a scan range from 10° to 40° 2θ, while the scanning speed was 4°/min.

Morphology was investigated using a differential scanning calorimeter (Perkin Elmer, DSC-4000, 2013). The sample (1.5 – 3.5 mg), in an aluminum Tzero pan, was heated at a scanning rate of 10 °C/min from –85 °C to 180 °C, quenched and then heated again. Dry N_2 was used as the purge gas at 50 ml/min. The instrument was equilibrated at –85 °C. Calibration of temperature and the cell constant was performed with indium. T_g was recorded as the mid-point of the endothermic step transition from the 2nd heat scan. Thermal transitions were viewed and analyzed using the analysis software Universal Analysis 2000.

Particles were stored for 2–3 weeks before analyzing with PXRD and DSC. The particles were kept in glass vials covered tightly with screw caps and stored in the refrigerator (~–20 °C).

2.2.7. *Dissolution studies*

Typically, an equivalent amount of free drug and nanoparticles was dispersed in 100 ml of potassium phosphate buffer at pH 6.8 (the pH of the human small intestine) for 5 hours at 37 °C. The apparatus used in the release experiments consisted of a beaker that was continuously shaken at 60 rpm in a water bath shaker at 37 °C. The mixture was constantly stirred at 200 rpm with a magnetic stir bar. Aliquots (0.8 ml) were withdrawn from the suspensions every 0.5 h for the first 2 hours and then every hour for 5 h. Phosphate buffer (pH 6.8, 0.8 ml) was added to maintain a constant volume after each aliquot was withdrawn. Samples were ultracentrifuged at 13,000 rpm (equivalent of 16,060 g) in an accuSpin Micro centrifuge (Fisher Scientific) for 10 min. The supernatant was recovered, and the solution concentration was determined by HPLC. The solubility studies were performed approximately 2–3 weeks after the preparation of the particles. The particles were kept in glass vials covered tightly with screw caps and stored in the refrigerator.

3. Results and discussion

The drug composition, size, crystallinity and solubility of the nanoparticles were investigated. The role of polymers in enhancing solubility and inhibiting drug crystallinity in the particles is also discussed.

3.1. *Drug incorporation in particles*

Nanoparticle RTV and EFV drug loadings are shown in Table 2. The calculations for wt% of drug (W_{drug}) and standard deviation of drug loading (σ_{wdrug}) were made using Equations (1) and (2). The dry powders (1 mg/ml concentration, i.e., 15 mg of powder dissolved in 15 ml of acetonitrile) of the drug-polymer were dissolved in acetonitrile and shaken for 15 min in a wrist-action shaker. The sample was placed in a quartz cuvette that was used for spectrophotometric measurements. The same cuvette was used to perform a baseline correction with pure acetonitrile before analyzing any samples. The drug (RTV or EFV) loading W_{Drug} for the dried particles (after dissolving in acetonitrile) is given by:

$$W_{Drug} = \frac{\begin{matrix}\textit{Final concentration of the Ritonavir}\\ \textit{or Efavirenz in the solvent}\\ \textit{Initial concentration of}\\ \textit{particles in the solvent}\end{matrix}}{} \times 100 = \frac{C_{drug}}{C_{part}} \times 100 \quad (1)$$

A sample calculation for the standard deviation of the drug loading σ_{WRTV} of the RTV-CMCAB nanoparticles is given by:

$$\sigma^2_{XRTV} = \sigma^2_{CRTV}\left(\frac{m_{Ace}}{\rho_{Ace}\, m_{comp}}\right)^2 + \sigma^2_{mAce}\left(\frac{C_{RTV}}{\rho_{Ace} m_{comp}}\right)^2 + \sigma^2_{mcomp}\left(\left(\frac{C_{RTV} m_{Ace}}{\rho_{Ace}}\right)\left(\frac{1}{m^2_{comp}}\right)\right)^2$$

$$\sigma_{W_{RTV}} = \sigma_{X_{RTV}} \times 100 \quad (2)$$

where:

σ_{XRTV} = standard deviation of mass fraction of RTV drug in the particles

σ_{wRTV} = standard deviation of weight fraction of RTV drug in the particles

m_{Ace} = mass of acetonitrile which is used to make samples

σ_{mAce} = standard deviation of the mass of acetonitrile used to make sample

σ_{mcomp} = standard deviation of the mass of the dried complexes

σ^2_{RTV} = standard deviation of the RTV concentration measured with the HPLC and is given by:

$$\sigma^2_{CRTV} = \sigma^2_{Abs}\left(\frac{1}{b}\right)^2 + \sigma^2_a\left(\frac{1}{b}\right)^2 + \sigma^2_b\left(\frac{Abs - a}{b^2}\right)^2$$

where:

σ_{Abs} = standard deviation of the absorbance measurement. This can be estimated from information about the typical uncertainty of the instrument's absorbance measurement. In this work, $\sigma_{Abs} \approx 0.004$ based on the HPLC manual.

a = y- intercept of the absorbance-calibration curve

b = slope of the absorbance-calibration curve

All samples showed good batch-to-batch reproducibility. There was some loss of free drug during certain processing

Table 2 – RTV and EFV composition in polysaccharide nanoparticles measured by HPLC at 240 nm. Average from three batches are shown.

	Drug composition (wt%) in CAP Adp 0.33 (standard deviation = σwdrug)	Drug composition (wt%) in CAP Adp 0.85 (standard deviation = σwdrug)	Drug composition (wt%) in CAP 320S Seb (standard deviation = σwdrug)	Drug composition (wt%) in CMCAB (standard deviation = σwdrug)
RTV	24 ± 0.02	22 ± 0.02	20 ± 0.01	19 ± 0.02
EFV	20 ± 0.01	19 ± 0.01	21 ± 0.01	18 ± 0.01

steps, such as the dialysis. Nanoparticle drug loading efficiency was comparable (88–96 %) for all cellulosic polymers. The cellulose derivatives are hydrophobic and are therefore able to retain more hydrophobic drug after processing. There were no significant differences between the trends for RTV and EFV loading in the particles.

3.2. *Particle size analysis*

The particle sizes were compared after each processing step to observe any significant changes in size due to individual processing steps. The particle sizes measured by DLS from all three processing steps for all drug compositions were 100–200 nm, with a polydispersity index of approximately 0.2. Fig. 1 shows the particle sizes after each processing step. The particle sizes were comparable after mixing and dialysis, with a standard deviation of approximately ±30 nm. Significant agglomeration was observed during freeze-drying, as observed in the sample without cryoprotectant. Several theories have been proposed to explain this effect, such as the crystal bridge theory, capillary pressure theory, hydrogen bond theory and chemical bond theory [34]. The aggregation of particles in this work is possibly due to ice crystal formation that repels foreign particles from the interstitials. During sublimation, the ice crystals leave microscopic pores. Another cause could be the drying of water, during which loss of electrostatic stabilization leads to particle–particle aggregation. Nanoparticles may become attached as a result of hydrogen bonds and/or connecting of surface hydroxyl groups. This can be reduced by using cryoprotectors such as glucose, sucrose, trehalose and mannitol. In this study, addition of trehalose before freezing at a weight ratio trehalose:nanoparticles of 1:10 resulted in a significant reduction in particle size and polydispersity index. It was observed that higher concentrations of trehalose resulted in smaller polydispersity index (PDI) values. It is important to note that trehalose was only used for particle size experiments and not for the drug dissolution experiments.

The microparticles were too large and too aggregated to be measured by dynamic light scattering and were instead characterized by FESEM. The microparticles formed agglomerated subunits of nearly spherical particles from 1–3 μm for CAP Adp 0.33-RTV microparticles and 2–8 μm for CAP Adp 0.85-RTV microparticles (Fig. 2).

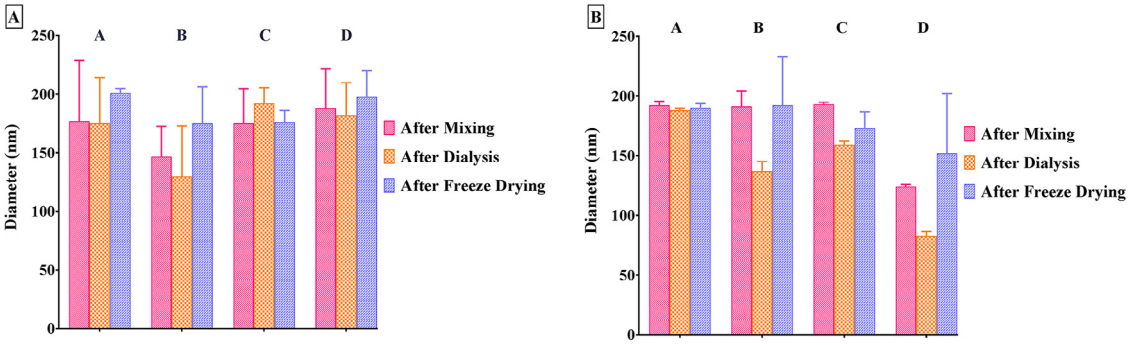

Fig. 1 – (A) Particle sizes of nanoparticles after mixing, dialysis and freeze drying. A, B, C and D in the graph represents nanoparticles prepared with CAP Adp 0.33-RTV, CAP Adp 0.85-RTV, CA 320S Seb-RTV, CMCAB-RTV respectively; (B) Particle sizes of nanoparticles after mixing, dialysis and freeze drying. A, B, C and D in the graph represents nanoparticles prepared with CAP Adp 0.33-EFV, CAP Adp 0.85-EFV, CA 320S Seb-EFV, CMCAB-EFV respectively.

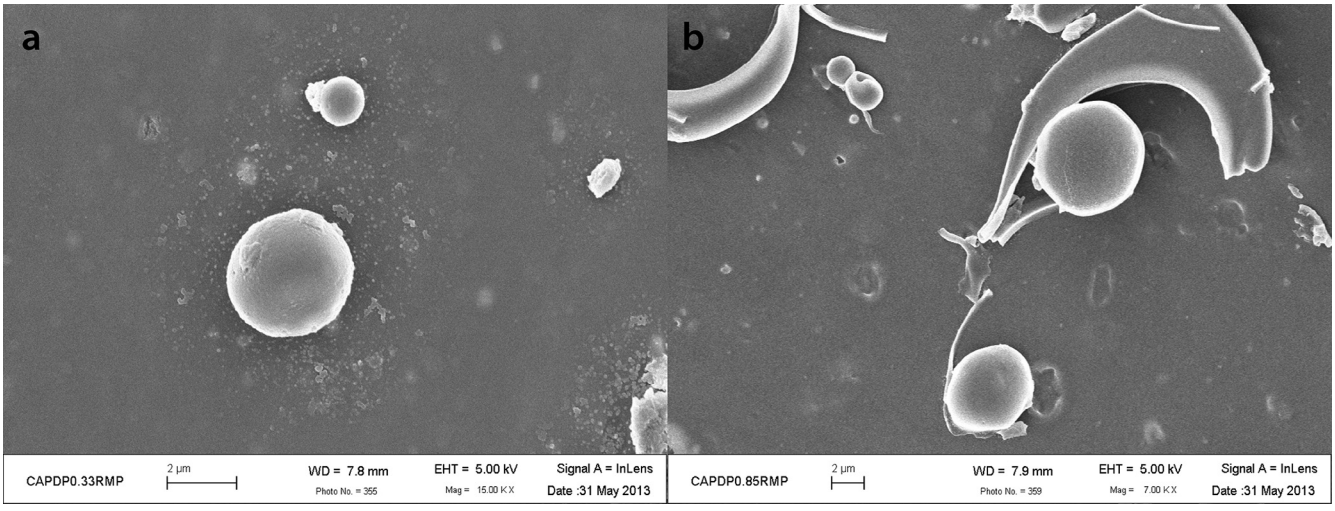

Fig. 2 – Scanning electron microscope images for (A) CAP Adp 0.33-RTV microparticles at 15Kx magnification, (B) CAP Adp 0.85-RTV microparticles at 7Kx magnification. The bar in each image corresponds to 2 μm.

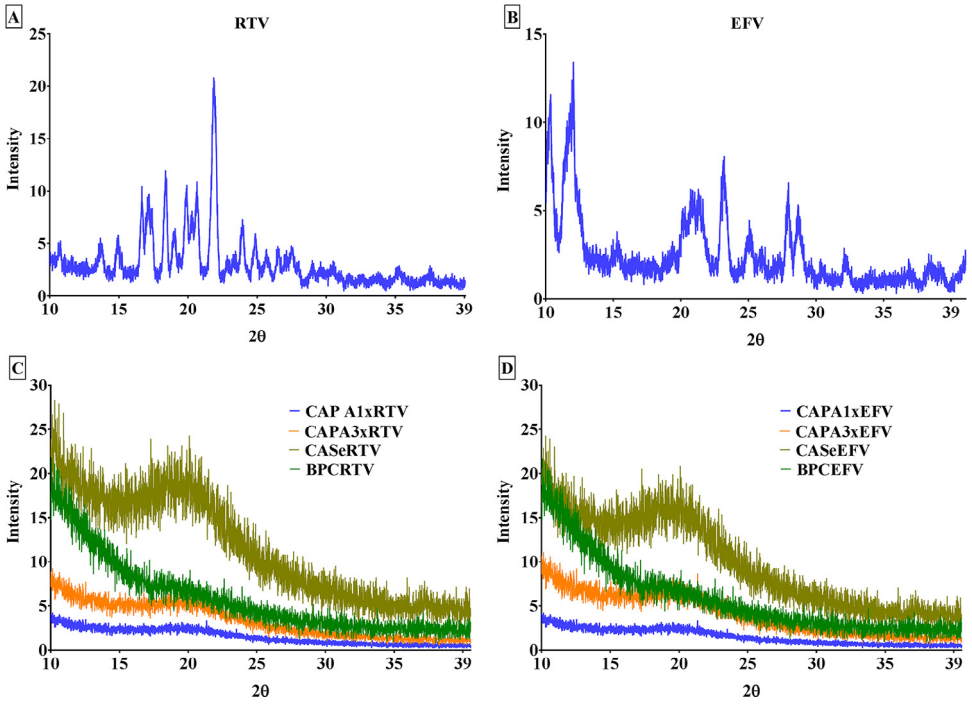

Fig. 3 – X-ray diffractograms of (A) Crystalline RTV (as received), (B) Crystalline EFV (as received) and polyssacharide nanoparticles (C) ascending order: CAP Adp 0.33-RTV, CAP Adp 0.85-RTV, CA 320S Seb-RTV, CMCAB-RTV, (D) ascending order: CAP Adp 0.33-EFV, CAP Adp 0.85-EFV, CA 320S Seb-EFV, CMCAB-EFV showed no diffraction peaks implying the drugs were mostly amorphous.

3.3. *Crystallinity of nanoparticles*

The influence of novel polysaccharides on possible phase transformation in RTV-polymer and EFV-polymer nanoparticles was investigated through X-ray diffraction. The PXRD pattern of the drugs showed distinctive peaks, as shown in Fig. 3A and 3B, along with results for the nanoparticles (Fig. 3C and 3D). The X-ray diffraction pattern for pure RTV drug showed numerous strong distinctive peaks at ~ 16°, 18°, 20°, 22° at 2θ, indicating a highly crystalline nature. The X-ray diffraction pattern for pure EFV drug also showed numerous strong distinctive peaks at 10°, 12°, 20°, 22°, 25°, 28° at 2θ, indicating its crystallinity. The polymers were amorphous in nature. Finally, the PXRD of the solid dispersions of the nanoparticles showed no diffraction peaks, indicating that they contained amorphous drug.

3.4. *Differential scanning calorimetry*

DSC scans for RTV, polymers and polymer-drug nanoparticles are shown in Fig. 4. Ritonavir showed a sharp melting peak at 126° C. During scanning of RTV-containing nanoparticles, no endotherm was observed near the melting point of ritonavir, indicating that ritonavir was present in an amorphous state. Similar results were obtained for polymer-EFV particles (not shown). The DSC curve with CMCAB was shown in a previous study [34] and is not included here.

The T_g values of RTV and EFV nanoparticles and their pure components are shown in Table 3. Glass transitions for the nanoparticles were between those of the polymers (between 105 °C–122 °C) and pure RTV (50° C) or EFV (34 °C). The intermediate T_g suggested that the drugs were homogeneously and molecularly dispersed in the amorphous polymer matrix.

It is helpful to study the amorphous forms of the drugs (RTV and EFV) in the solid dispersions by measuring the glass transition temperature of the solid dispersion. Such measurements can establish whether the drug and polymer form a single miscible phase (i.e., a single T_g value, solid dispersion) or immiscible phases (i.e., multiple T_g values, glassy suspension) [35,36]. All results in Table 3 show the presence of a single glass transition temperature, suggesting that the drug and polymer formed a miscible amorphous phase. However, the glass transition temperatures of some of the drug-containing nanoparticles are similar to those of the drugs. This can pose storage problems, as it is known that storage temperatures 50 °C below the

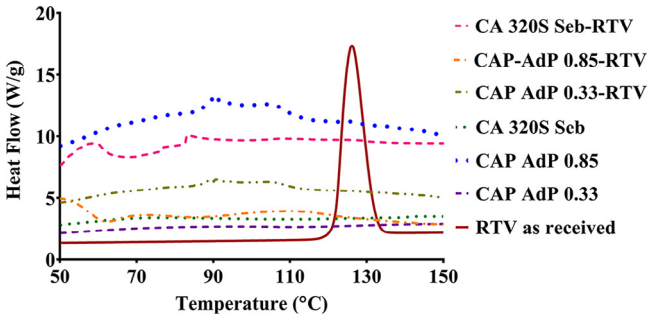

Fig. 4 – First DSC scan showing melting peak of RTV at 126°C. No such peak are observed in any of the polymer-drug nanoparticles.

Table 3 – Glass transitions of polymer, drugs and polymer-drug nanoparticles (2nd DSC scans).

Samples	No Drugs	RTV (Drug loading)	EFV (Drug loading)
	T_g (°C)	T_g (°C) (wt%)	T_g (°C) (wt%)
CAP Adp 0.33	**122**	64 (24)	51 (20)
CAP Adp 0.85	**105**	55 (22)	42 (19)
CA-320S Seb	**111**	52 (20)	47 (21)
CMACB	**137**	91 (19)	99 (18)
RTV as received	-	**51**	-
EFV as received	-	-	**35**

Tg reduce mobility sufficiently to allow acceptable physical stability [13,37]. In the absence of polymer, indomethacin recrystallized in less than six weeks at storage temperatures 20 °C below the T_g. However, when the drug was molecularly dispersed in PVP solid dispersions, the difference between the Tg of indomethacin in the formulations and the storage temperature increased to 40–50 °C, and recrystallization of indomethacin was suppressed [38]. Such low glass transitions may not be suitable for storage. Even though the nanoparticles did not show much of an increase in T_g compared to the pure drug, they did not show phase separation in the solid state (DSC, XRD) or drug re-crystallization upon storage in three weeks before the characterizations were performed. CMCAB proved to be the best polymer for drug stabilization from recrystallization and was suitable for storage.

3.5. *Dissolution studies*

The results from the dissolution experiment showed good enhancement of drug solution concentrations from the nanoparticles. There was an almost 10–20-fold increase in the solubility of RTV (Fig. 5A) and EFV (Fig. 5B) from cellulose derivatives compared to the crystalline drug alone. Among the cellulose derivatives, the CAP Adp 0.33 showed a smaller increase in solubility compared to the others, with respect to the free drug. However, there was not much difference in the solubility concentration among the cellulose derivatives. CMCAB showed the best results among all the polymers.

The solubility parameters (SP) shown in Table 1 dictate the relative hydrophobicities of the novel polymers. The method proposed by Fedors was used to estimate the SP [39], which provides a numerical assessment of the intermolecular forces within a material and can be a good indication of solubility [32] . Higher SP indicates a more hydrophilic material. For hydrophobic polymers (CAP Adp 0.33, CAP Adp 0.85 and CA 320S Seb), the SP lies between 20.56–22.36 $MPa^{1/2}$.

The amorphous blends with cellulose derivatives significantly increased the solubility of both RTV and EFV, and the supersaturated solutions remained stable with respect to drug re-precipitation over the course of the experiment. This suggests that the polymers not only stabilized the amorphous drugs in the solid state but also helped stabilize the dissolved drugs in solution.

The percent drug release from the particles was calculated using equation 3 for RTV and EFV.

$$\%\ drug\ release = \frac{C_{experimental}}{C_{theoritical}} \quad (3)$$

$C_{experimental}$ was obtained from HPLC and $C_{theoretical}$ was calculated from the known volumes of the buffer solution, the mass of particles and drug composition.

Drug release was studied for up to five hours as shown for RTV (Fig. 6A) and EFV (Fig. 6B). CAP Adp 0.33 released approximately 20% of RTV, CAP Adp 0.85 released 27% of RTV and CA 320S Seb released 30% of RTV within five hours. There was not much difference in the release profile of EFV from the polymer. However, CMCAB showed the highest release (up to 40%) of the drugs.

The rate of dissolution for solid drug products can be enhanced by particle size reduction, thereby increasing the surface area per unit mass available for solvation. Particle size reduction techniques are routinely used to improve the oral bioavailability of drugs with poor water solubility [40]. In this study, the increase in surface area generated due to formation of nanoparticles increases dissolution and therefore potentially increases the bioavailability for drugs where exposure after oral administration is limited by dissolution rate. Drug release can be correlated to polymer solubility parameters.

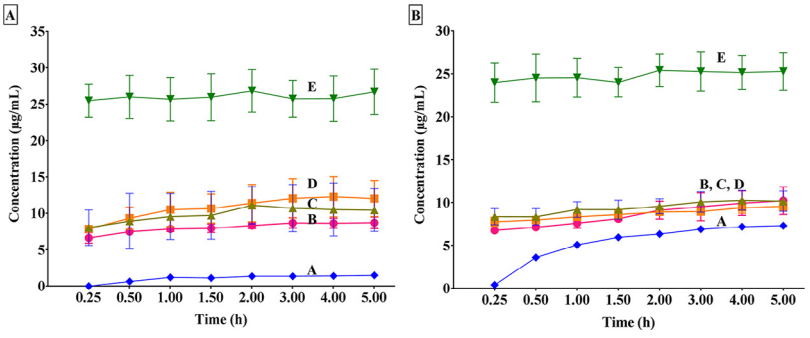

Fig. 5 – (A) Concentration profile of RTV: A – as received, B – from CAP Adp 0.33, C – from CA 320S Seb, D – from CAP Adp 0.85, E – from CMCAB; (B) Release profile of EFV: A – as received, B – from CAP Adp 0.33, C – from CAP Adp 0.85, D – from CA 320S Seb, E – from CMCAB. The error bars represents standard deviation of results from 3 batches.

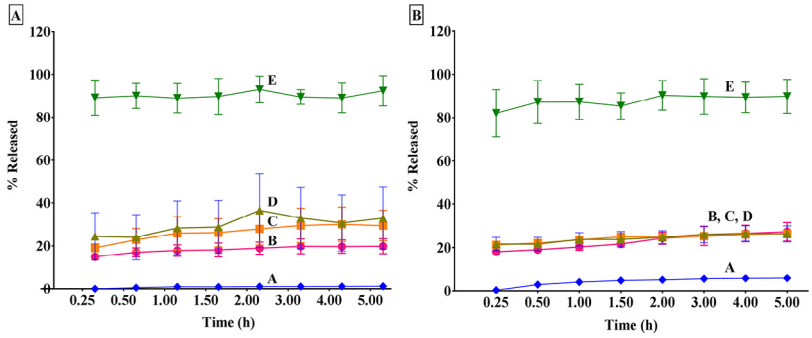

Fig. 6 – (A) Release profile of RTV: A – as received, B – from CAP Adp 0.33, C – from CAP Adp 0.85, D – from CA 320S Seb, E – from CMCAB; (B) Release profile of EFV: A – as received, B – from CAP Adp 0.33, C – from CAP Adp 0.85, D – from CA 320S Seb, E – from CMCAB. The error bars represent standard deviation of results from 3 batches.

CAP Adp 0.33 has the lowest solubility parameter among the four cellulose derivatives studied and therefore is more hydrophobic, whereas CMCAB is comparatively more hydrophilic, as it has a higher solubility parameter and provides higher RTV solution concentrations. These polymers have been shown to be effective in inhibiting RTV recrystallization [41] . Polymers with solubility parameters between 20–23 $MPa^{1/2}$ could inhibit crystal growth in solution, whereas polymers with a solubility parameter below 20 were mostly ineffective. Hydrophobicity is likely to affect the extent of adsorption of polymer to the crystal surface, which in turn influences its effectiveness. If the polymer is very hydrophobic, it is expected to interact more favorably with other monomer units to form a more condensed globule. This globule may not adsorb onto the crystal, or if it adsorbs, may not have high surface coverage. If the polymer is very hydrophilic, it can interact more with water and comparatively less with the drug. Therefore, an optimal hydrophobicity for inhibiting crystallization may exist. Previous work has shown that ionizable carboxylic acids (evaluated by DS) are effective inhibitors of RTV crystallization [41] . The substituent group here such butyryl, acetyl, propionate imparts amphiphilic nature to the polymer depending on the ionic groups, hydrogen bonding present in them. DS is not solely responsible for dissolution or inhibition of crystallinity, but combined factors such as hydrophobicity, rigidity and amphiphilic nature of the novel cellulose-based polymers on crystal growth inhibition. Our findings had similar characteristics in accord with previous studies.

3.5.1. *Comparison of drug solubility and release from nanoparticles and microparticles*

The solubility characteristics and percent drug release of RTV from nanoparticles and microparticles (prepared by co-precipitation) of representative cellulose adipate derivatives (CAP Adp 0.33 and CAP Adp 0.85) are compared. The solution concentration of the drug was enhanced approximately six-fold and eight-fold for CAP Adp 0.33 and CAP Adp 0.85, respectively, compared to crystalline RTV. The solution concentration of RTV from nanoparticles was slightly higher than from corresponding microparticles, but within the margin of error.

There was an increase in the release of drugs from both nanoparticles and microparticles. RTV was released (approximately 15% from CAP Adp 0.33 and 19 % from CAP Adp 0.85)

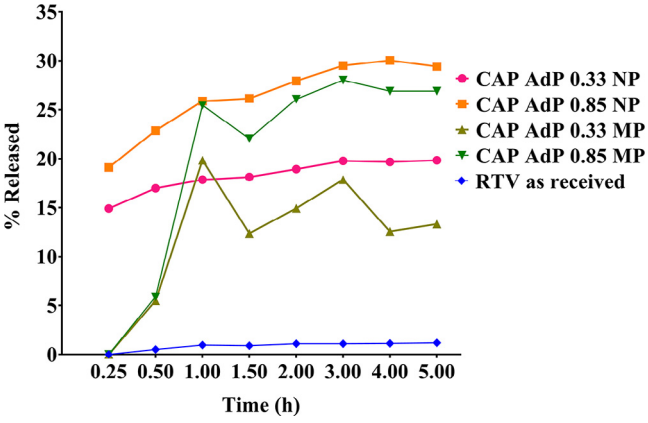

Fig. 7 – Comparison of RTV release from CAP Adp 0.33 and CAP Adp 0.85 microparticles (MP) and nanoparticles (NP), vs crystalline RTV (result from 1 batch). RTV compositions are listed in Table 2.

from nanoparticles within 15 min after the particles were dispersed in buffer but no drug was released from the microparticles during that time; drug release from microparticles was only observed after half an hour (Fig. 7). The much higher specific surface area of the nanoparticles resulted in an enhanced early dissolution rate of RTV compared to the microparticles. Approximately 19% and 30% of RTV was released from CAP Adp 0.33 and CAP Adp 0.85 after five hours.

4. Conclusions

This study demonstrates a method for producing cellulose derivative nanoparticles containing RTV and EFV with well-defined sizes (100 nm–200 nm). A multi-inlet vortex mixer was used to control the particle size and nucleation rate, and flash nanoprecipitation was shown to be an effective method for making these nanoparticles. The particles were processed by dialysis followed by freeze-drying; the cryoprotectant trehalose was used to inhibit particle aggregation during freeze-drying. The drug loading efficiency of the final particles was 88–96%. The polymers effectively entrapped the drugs in an

amorphous state in the particle, which in turn increased the solubility of the drugs in the buffer solution. There was an increase in percent drug release from nanoparticles compared to pure crystalline drug. The microparticles containing RTV and EFV showed peak/trough fluctuations in solubility and drug release values compared to nanoparticles, which showed a comparatively steady pattern. Therefore, nanoparticles of polysaccharides-drug complexes showed the potential for enhancing the solubility and sustained release of poorly soluble drugs (RTV and EFV). The dissolution behavior was dependent on the particle size and properties of the polymer (solubility parameter, degree of substitution, hydrophobicity) as well as the drug (solubility parameter, solubility, presence of hydrophobic groups). Therefore, an optimal hydrophobicity may exist for inhibiting crystallization. A higher degree of substitution (DS) shows more effective inhibition of crystallization (more ionizable carboxylic acids can better inhibit crystal growth). The particle shape, size, polydispersity and morphology vary with preparation method, and thus, care must be taken in the synthesis and purification (separation, drying) techniques to obtain well-defined particles. The use of excipients, such as cryoprotectants (or excipients), to control the particle size would be a useful additional step. This study showed synergy between a high surface area (due to nanoparticles) and suppression of crystallinity (due to amorphous dispersions of cellulose acetate matrix) in enhancing the dissolution of poorly soluble drugs.

Conflicts of interest

The authors declare that there are no conflicts of interest.

Acknowledgment

This work is supported by Research Initiation Grant, BITS Pilani, Pilani campus, India. The authors gratefully acknowledge Department of Chemical Engineering and Department of Pharmacy, BITS Pilani for assisting with analytical measurements.

REFERENCES

[1] Lavelle EC, Sharif S, Thomas NW, et al. The importance of gastrointestinal uptake of particles in the design of oral delivery systems. Adv Drug Deliv Rev 1995;18:5–22.
[2] Daugherty AL, Mrsny RJ. Regulation of the intestinal epithelial paracellular barrier. Pharm Sci Technolo Today 1999;2:281–287.
[3] Gaucher G, Satturwar P, Jones M-C, et al. Polymeric micelles for oral drug delivery. Eur J Pharm Biopharm 2010;76:147–158.
[4] Merisko-Liversidge E, Liversidge GG, Cooper ER. Nanosizing: a formulation approach for poorly-water-soluble compounds. Eur J Pharm Sci 2003;18:113–120.
[5] Meenakshi BDK, Harish D, Vivek K. Nanoparticle technology for the delivery of poorly water-soluble drugs. Pharm Technol 2006;30:1–11.
[6] Chan JM, Valencia PM, Zhang L, et al. Polymeric nanoparticles for drug delivery. In: Grobmyer SR, Moudgil BM, editors. Cancer nanotechnology: methods and protocols. Totowa, NJ: Humana Press; 2010. p. 163–175.
[7] Gao Y, Carr RA, Spence JK, et al. A pH-Dilution method for estimation of biorelevant drug solubility along the gastrointestinal tract: application to physiologically based pharmacokinetic modeling. Mol Pharm 2010;7:1516–1526.
[8] Kennedy M, Hu J, Gao P, et al. Enhanced bioavailability of a poorly soluble VR1 antagonist using an amorphous solid dispersion approach: a case study. Mol Pharm 2008;5:981–993.
[9] Law D, Schmitt EA, Marsh KC, et al. Ritonavir–PEG 8000 amorphous solid dispersions: *in vitro* and *in vivo* evaluations. J Pharm Sci 2004;93:563–570.
[10] Li S, Liu Y, Liu T, et al. Development and in-vivo assessment of the bioavailability of oridonin solid dispersions by the gas anti-solvent technique. Int J Pharm 2011;411:172–177.
[11] Newman A, Knipp G, Zografi G. Assessing the performance of amorphous solid dispersions. J Pharm Sci 2012;101:1355–1377.
[12] Van Eerdenbrugh B, Van Speybroeck M, Mols R, et al. Itraconazole/TPGS/Aerosil®200 solid dispersions: characterization, physical stability and in vivo performance. Eur J Pharm Sci 2009;38:270–278.
[13] Hancock BC, Parks M. What is the true solubility advantage for amorphous pharmaceuticals? Pharm Res 2000;17:397–404.
[14] Konno H, Taylor LS. Influence of different polymers on the crystallization tendency of molecularly dispersed amorphous felodipine. J Pharm Sci 2006;95:2692–2705.
[15] Florence ATAD. Physicochemical principles of pharmacy. 3rd ed. London: MacMillan; 1998.
[16] Ginés JM, Arias MJ, Moyano JR, et al. Thermal investigation of crystallization of polyethylene glycols in solid dispersions containing oxazepam. Int J Pharm 1996;143:247–253.
[17] Posey-Dowty JD, Watterson TL, Wilson AK, et al. Zero-order release formulations using a novel cellulose ester. Cellulose 2007;14:73–83.
[18] Shelton MC, Posey-Dowty JD, Lingerfelt L, et al. Enhanced dissolution of poorly soluble drugs from solid dispersions in carboxymethylcellulose acetate butyrate matrices. Polysaccharide materials: performance by design. J Am Chem Soc 2009;93–113.
[19] Dembri A, Montisci M-J, Gantier JC, et al. Targeting of 3′-Azido 3′-Deoxythymidine (AZT)-Loaded Poly(Isohexylcyanoacrylate) nanospheres to the gastrointestinal mucosa and associated lymphoid tissues. Pharm Res 2001;18:467–473.
[20] Destache CJ, Belgum T, Christensen K, et al. Combination antiretroviral drugs in PLGA nanoparticle for HIV-1. BMC Infect Dis 2009;9:198.
[21] Löbenberg R, Maas J, Kreuter J. Improved body distribution of 14C-labelled AZT bound to Nanoparticles in Rats determined by Radioluminography. J Drug Target 1998;5:171–179.
[22] Mainardes RM, Gremião MPD, Brunetti IL, et al. Zidovudine-loaded PLA and PLA–PEG blend nanoparticles: influence of polymer type on phagocytic uptake by polymorphonuclear cells. J Pharm Sci 2009;98:257–267.
[23] Sharma P, Garg S. Pure drug and polymer based nanotechnologies for the improved solubility, stability, bioavailability and targeting of anti-HIV drugs. Adv Drug Deliv Rev 2010;62:491–502.

[24] Johnson BK, Prud'homme RK. Mechanism for rapid self-assembly of block copolymer nanoparticles. Phys Rev Lett 2003;91:118302.
[25] Johnson BK, Prud'homme RK. Chemical processing and micromixing in confined impinging jets. AIChE J 2003;49:2264–2282.
[26] Johnson BK, Saad W, Prud'homme RK. Nanoprecipitation of pharmaceuticals using mixing and block copolymer stabilization. Polymeric drug delivery II. J Am Chem Soc 2006;278–291.
[27] Ansell SM, Johnstone SA, Tardi PG, et al. Modulating the therapeutic activity of nanoparticle delivered paclitaxel by manipulating the hydrophobicity of prodrug conjugates. J Med Chem 2008;51:3288–3296.
[28] Chen T, D'Addio SM, Kennedy MT, et al. Protected Peptide nanoparticles: experiments and brownian dynamics simulations of the energetics of assembly. Nano Lett 2009;9:2218–2222.
[29] Addio D, Prud SM, Homme RK. Controlling drug nanoparticle formation by rapid precipitation. Adv Drug Deliv Rev 2011;63:417–426.
[30] Kumar V, Hong SY, Maciag AE, et al. Stabilization of the Nitric Oxide (NO) Prodrugs and Anticancer Leads, PABA/NO and Double JS-K, through Incorporation into PEG-Protected Nanoparticles. Mol Pharm 2010;7:291–298.
[31] Liu Y, Cheng C, Liu Y, et al. Mixing in a multi-inlet vortex mixer (MIVM) for flash nano-precipitation. Chem Eng Sci 2008;63:2829–2842.
[32] Liu H, Ilevbare GA, Cherniawski BP, et al. Synthesis and structure–property evaluation of cellulose ω-carboxyesters for amorphous solid dispersions. Carbohydr Polym 2014;100:116–125.
[33] Chopra M, Jain R, Dewangan AK, et al. Design of curcumin loaded polymeric nanoparticles-optimization, formulation and characterization. J Nanosci Nanotechnol 2016;16:9432–9442.
[34] Vedula VB, Chopra M, Joseph E, et al. Preparation and characterization of nanoparticles of carboxymethyl cellulose acetate butyrate containing acyclovir. Appl Nanosci 2016;6:197–208.
[35] Marsac PJ, Konno H, Rumondor ACF, et al. Recrystallization of nifedipine and felodipine from amorphous molecular level solid dispersions containing poly(vinylpyrrolidone) and sorbed water. Pharm Res 2008;25:647–656.
[36] Qian F, Huang J, Hussain MA. Drug–polymer solubility and miscibility: stability consideration and practical challenges in amorphous solid dispersion development. J Pharm Sci 2010;99:2941–2947.
[37] Shamblin SL, Hancock BC, Dupuis Y, et al. Interpretation of relaxation time constants for amorphous pharmaceutical systems. J Pharm Sci 2000;89:417–427.
[38] Yoshioka M, Hancock BC, Zografi G. Inhibition of indomethacin crystallization in poly(vinylpyrrolidone) coprecipitates. J Pharm Sci 1995;84:983–986.
[39] Fedors RF. A method for estimating both the solubility parameters and molar volumes of liquids. Polym Eng Sci 1974;14:147–154.
[40] Kohane DS. Microparticles and nanoparticles for drug delivery. Biotechnol Bioeng 2007;96:203–209.
[41] Ilevbare GA, Liu H, Edgar KJ, et al. Understanding polymer properties important for crystal growth inhibition – impact of chemically diverse polymers on solution crystal growth of ritonavir. Cryst Growth Des 2012;12:3133–3143.